

## PAPER • OPEN ACCESS

## A compound Kinoform/Fresnel zone plate lens with 15 nm resolution and high efficiency in soft x-ray

To cite this article: Xujie Tong *et al* 2023 *Nanotechnology* **34** 215301

View the [article online](#) for updates and enhancements.

### You may also like

- [Direct electron beam writing of kinoform micro-axicon for generation of propagation-invariant beams with long non-diffracting distance](#)  
X-C Yuan, B P S Ahluwalia, W C Cheong et al.
- [QR code optical encryption using spatially incoherent illumination](#)  
P A Cheremkhin, V V Krasnov, V G Rodin et al.
- [Comparative simulations of Fresnel holography methods for atomic waveguides](#)  
V A Henderson, P F Griffin, E Riis et al.



**UNITED THROUGH SCIENCE & TECHNOLOGY**

**ECS** The Electrochemical Society  
Advancing solid state & electrochemical science & technology

**248th ECS Meeting**  
**Chicago, IL**  
October 12-16, 2025  
*Hilton Chicago*

**Science + Technology + YOU!**

**SUBMIT ABSTRACTS by March 28, 2025**

**SUBMIT NOW**

The banner features a woman in a tan blazer smiling and gesturing towards the right. The background is blue with circular patterns resembling molecular structures. A red button at the bottom right says "SUBMIT NOW".

# A compound Kinoform/Fresnel zone plate lens with 15 nm resolution and high efficiency in soft x-ray

Xujie Tong<sup>1</sup>, Yifang Chen<sup>1</sup> , Chengyang Mu<sup>1</sup>, Qiucheng Chen<sup>1</sup>, Xiangzhi Zhang<sup>2</sup>, Guang Zeng<sup>3</sup>, Yuchun Li<sup>3</sup>, Zijian Xu<sup>2</sup>, Jun Zhao<sup>1,2</sup>, Xiangjun Zhen<sup>2</sup>, Chengwen Mao<sup>2</sup>, Hongliang Lu<sup>3</sup>  and Renzhong Tai<sup>2</sup>

<sup>1</sup> Nanolithography and Application Research Group, School of Information Science and Technology, Fudan University, Shanghai 200433, People's Republic of China

<sup>2</sup> Shanghai Synchrotron Radiation Facility, Shanghai Advanced Research Institute, Chinese Academy of Sciences, Shanghai 201210, People's Republic of China

<sup>3</sup> State Key Laboratory of ASIC and System, Shanghai Institute of Intelligent, Electronics & Systems, School of Microelectronics, Fudan University, Shanghai 200433, People's Republic of China

E-mail: [yifangchen@fudan.edu.cn](mailto:yifangchen@fudan.edu.cn)

Received 7 October 2022, revised 19 January 2023

Accepted for publication 6 February 2023

Published 7 March 2023



## Abstract

X-ray microscope as an important nanoprobing tool plays a prevailing role in nano-inspections of materials. Despite the fast advances of high resolution focusing/imaging reported, the efficiency of existing high-resolution zone plates is mostly around 5% in soft x-ray and rapidly goes down to 1%–2% when the resolution approaches 10 nm. It is well known that the rectangular zone shape, beamstop, limited height/width ratios, material absorption of light and structural defects are likely responsible for the limited efficiency. Although zone plates with Kinoform profile are supposed to be efficient, progress for achieving both high resolution (<30 nm) and high efficiency (>5%) have hardly been addressed in soft x-ray. In this work, we propose a compound Kinoform/Fresnel zone plate (CKZP) by combining a dielectric Kinoform zone plate with a 15 nm resolution zone plate. Greyscale electron beam lithography was applied to form the 3D Kinoform zone plate and atomic layer deposition was carried out to form the binary zone plate. Optical characterizations demonstrated 15 nm resolution focusing/imaging with over 7.8% efficiency in soft x-ray. The origin of the efficiency improvement behind the proposed compound lens is theoretically analyzed and discussed.

Supplementary material for this article is available [online](#)

Keywords: dielectric kinoform zone plate, grayscale electron beam lithography, atom layer deposition, beam propagation method (BPM), high efficiency focusing in soft x-ray

(Some figures may appear in colour only in the online journal)

## 1. Introduction

Extensive applications of x-ray microscopy in bio-science [1–7] demand fast advances of soft x-ray lenses (0.2–2 keV)

such as Fresnel zone plates as critical components in x-ray nanoprobe toward high resolution and high efficiency. In the past decades, high resolution zone plates have been frequently reported [8–11]. Especially, Vila-Comamala [12] proposed a zone-doubled Fresnel zone plate of 15 nm resolution with 7.5% focusing efficiency in hard x-ray (6.2 keV) by atomic layer deposition (ALD) of a 15 nm Ir film as the outer zones [13, 14]. Based on the same tactics, zone plates with 10 nm or even sub-10 nm resolution [15, 16] in soft x-ray has been



Original content from this work may be used under the terms of the [Creative Commons Attribution 4.0 licence](#). Any further distribution of this work must maintain attribution to the author(s) and the title of the work, journal citation and DOI.

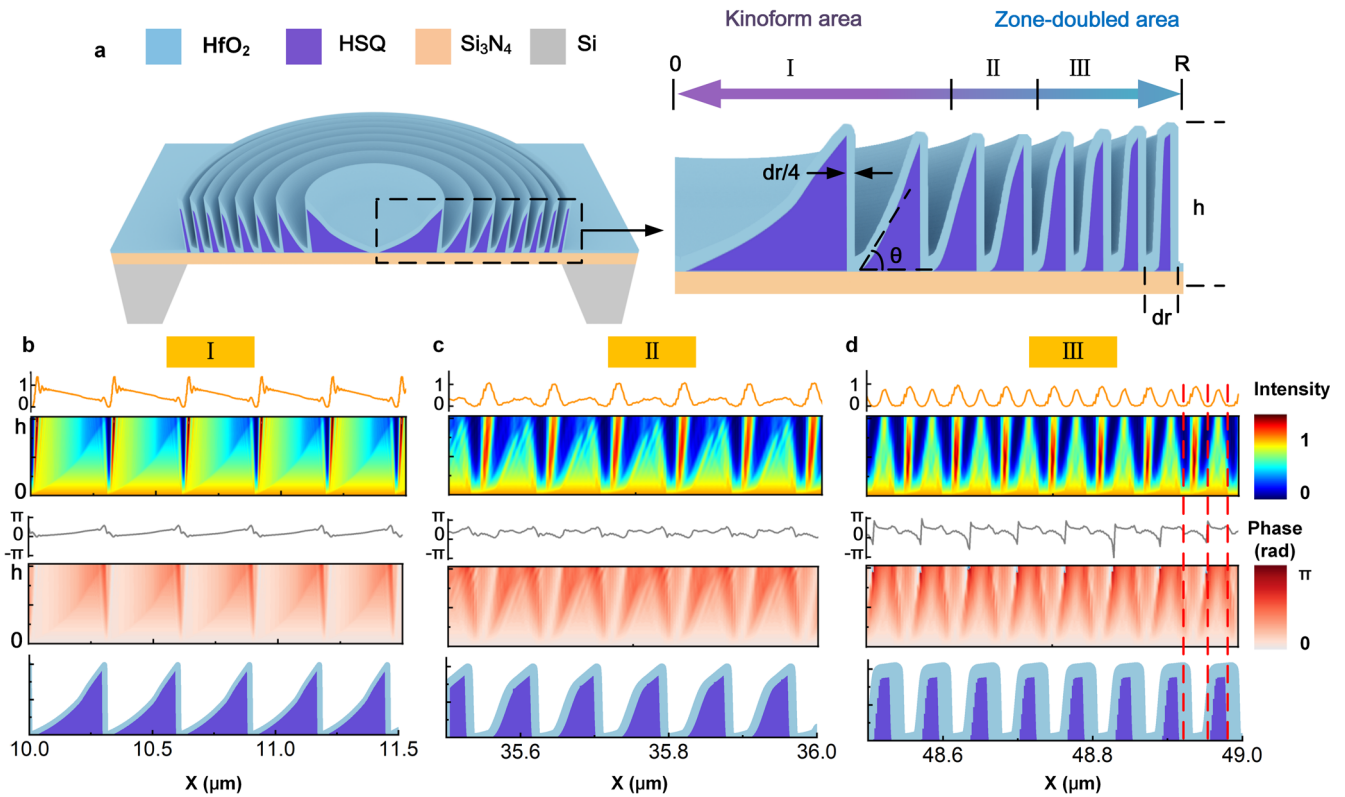


**Figure 1.** Illustration of the compound Kinoform/Fresnel zone plate in soft x-ray and the wave field propagation inside the lens. (a) Illustrations of zone profile for the HfO<sub>2</sub>-HSQ-CKZP. The HSQ Kinoform zone plate is coated with a thin HfO<sub>2</sub> with the thickness of  $Dr/4$ . The lens is divided into three regions according to the slope of replicated ridges (I:  $0 < \theta < 70^\circ$ ; II:  $70 < \theta < 80^\circ$ ; III:  $80 < \theta < 90^\circ$ ). (b)–(d) The zone profiles in three different regions are shown at the bottom panel, respectively. Corresponding 2D intensity (top panel) and phase (middle panel) distribution of the wave field inside the HfO<sub>2</sub>-HSQ-CKZP ( $R = 50 \mu\text{m}$ ,  $Dr = 60 \text{ nm}$ ,  $h = 350 \text{ nm}$ ) are presented, calculated by beam propagation method with x-ray energy of 1200 eV. The 1D wave field intensity (orange solid line) and the phase (grey solid line) variation at exit surface are attached to the 2D maps, respectively.

reported, but the efficiency is not yet encouraging because of the large beamstop in the centre and the rectangular zone shape [15, 17].

It is understood that Kinoform zone plates (KZPs) with parabolic zone profile are able to realize high efficiency focusing by manipulating continuous phase shift [18]. Efficiency up to 53% with the resolution of 200 nm was reported [19]. However, it becomes technically unfeasible to maintain parabolic shape for the outer zones with the width approaching 100 nm or even narrower [20–22]. A combined focusing scheme of a Fresnel zone plate was therefore proposed by Simpson and Michette [23], that is the first-order foci of the inner zones was designed to coincide with the third-order foci of the outer zones, trying to realize enhancements in both resolution and focusing efficiency.

Inspired by the existing achievements as mentioned above, this paper reports our recent progress in developing a compound Kinoform/Fresnel zone plate lens (CKZP) in soft x-ray, that is to combine a Kinoform shaped zone plate with a regular one in outer zones. Beam Propagation Method (BPM) [24, 25] was utilized to model the focusing performance for optimizing the 3D profile of inner zones. State-of-art 3D greyscale electron beam lithography (GS-EBL) was applied to generate the desired Kinoform shape. Zone doubling technique [12] was exploited to

form the outer zones with 15 nm resolution. Optical characterizations of the lens were carried out by scanning transmission x-ray microscope in Shanghai Synchrotron Radiation Facilities (SSRF) and the efficiency contributions from each part of the compound lens are calculated and discussed.

## 2. Focusing performance modeling of the compound Kinoform/Fresnel zone plate

Figure 1(a) schematically illustrates the compound Kinoform/Fresnel zone plate with the radius of  $R$ , in which the purple color depicts the Kinoform zone plate with the outermost zone-width of 15 nm, generated by electron beam lithography (EBL) on SiO<sub>x</sub>-based hydrogen silsesquioxane (HSQ). The whole lens can be radially divided into three regions according to the slope of replicated ridges (region I:  $0 < \theta < 70^\circ$ ; region II:  $70 < \theta < 80^\circ$ ; region III:  $80 < \theta < 90^\circ$ ). Region-I (0–0.5R) is for the inner zones with typical Kinoform profile, replicated by greyscale EBL (GS-EBL) following the simulated topography using BEAMER/TRACER/LAB software (GenLSys Ltd). Region-II (0.5R–0.7R) is for the middle zones with the transitional profile from Kinoform to rectangular shape. Region III (0.7R–1.0R) is for the outer zones with the outermost zone-width of 30 nm but the actually

patterned line-width is 15 nm with the pitch of 60 nm. Apparently, almost all the zones in region-III are rectangular shaped.

The grey color in figure 1(a) is the 15 nm thick HfO<sub>2</sub> film, which is grown by atomic layer deposition (ALD) on the surface or sidewalls of the replicated Kinoform zone plate (see Supplement 1 for specific dose parameters). In both region-I and region-II, the HSQ-Kinoform zone plate is expected to behave like a refractive lens, and the 15 nm thick HfO<sub>2</sub> should contribute negligible effect on the light focusing/imaging. In region-III, however, the HfO<sub>2</sub> film on the sidewalls of replicated HSQ lines forms a rectangular zone plate with the resolution of 15 nm. Therefore, the compound Kinoform/Fresnel zone plate is the combination of the HSQ-Kinoform zone plate (region-I + region-II + region-III) and the HfO<sub>2</sub> zone plate in region-III.

The propagation of wavefield inside the zones was calculated using our modified Beam Propagation Method [25] based on a radial 2D model of the compound Kinoform/Fresnel zone plate (CKZP) by MATLAB. The calculated two-dimensional (2D) phase and the intensity distribution of the actual wave field inside the HSQ-Kinoform/HfO<sub>2</sub> zone plate is presented in figures 1(b) and (d), respectively. The detailed calculation process can be found in [25]. One-dimensional (1D) phase (grey solid line) and the intensity (orange solid line) variation of the wavefield on the exit surface is shown on the top of each 2D map. The simulated zone profiles are presented as the reference at the bottom of figure 1. As shown in region-I in figure 1(b), the wavefield inside the Kinoform zones has continuous phase shift, indicating that the HSQ-Kinoform zones work in refractive mode. The effect of the 15 nm thick HfO<sub>2</sub> on the top in this region is negligible due to the limited thickness along the optical path. In region-II (figure 1(c)), intensity peaks can be observed at the exit of each zone together with interrupted phases, which is mainly caused by the competition between diffractive waves on the HfO<sub>2</sub>-HSQ boundary and refractive waves in the HSQ-Kinoform zones. In region-III, diffraction becomes dominant and all the intensity peaks correspond to HfO<sub>2</sub> zones, as shown in figure 1(d), indicating that the vertical HfO<sub>2</sub> zones work as a diffractive zone plate with 15 nm resolution.

Based on the calculated wavefronts at the exits of the three zone regions as presented in figure 1(b)–(d), the focusing performance of the compound lens can be calculated. The wavefield propagation in free space along the optical axis was obtained by the 0th order Hankel transform [26] and BPM [25] for three different zone plates, i.e. the HSQ-Kinoform zone plate, the binary HfO<sub>2</sub>-zone plate and the compound HSQ-Kinoform/HfO<sub>2</sub>-zone plate, respectively, as shown in figure 2. It can be seen that the intensity of the 1st order focus with 30 nm resolution by the refractive HSQ-Kinoform zone plate (figure 2(a)) is very high thanks to its low loss material (HSQ). The 2nd order foci with the resolution of 15 nm at the distance of 1.5 mm can also be identified, which is caused by the nonideal parabolic profile of the zones as numerically simulated by the lithographic software. Figure 2(b) presents the light field propagation through the

binary HfO<sub>2</sub>-zone plate (the outmost zone width is 15 nm) with the 1st order focus at 1.5 mm, which coincides with the second order foci of the HSQ-Kinoform lens. In the calculation, a beamstop with the diameter of 40  $\mu\text{m}$  was used to block the light through the central area. When combining the HSQ-Kinoform zone plate (HSQ-KZP) with the 15 nm resolution HfO<sub>2</sub>-zone plate (HfO<sub>2</sub>-ZP) together to form the compound one, the focusing intensity in the 2nd order focal plane at 1.5 mm is the superposition of the ones, respectively by the 2nd order focus of the HSQ-KZP and the 1st order focus of the HfO<sub>2</sub>-ZP, giving rise to 2–3 times enhanced intensity with 15 nm resolution. Therefore, the 2nd order focus at 1.5 mm should be the best working distance for the proposed compound Kinoform/Fresnel zone plate.

In addition to the structural study, the materials of the compound lens were also compared. Figure 2(e) presents the calculated efficiencies of the compound Kinoform/Fresnel zone plate ( $R = 50 \mu\text{m}$ ,  $D_r = 60 \text{ nm}$ ,  $h = 350 \text{ nm}$ ) with various metals and oxides. Due to relatively large phase shifts ( $1 - \delta$ ) and low absorption ( $\beta$ ) for metal oxides, compound lenses with ALD-HfO<sub>2</sub> or ALD-Al<sub>2</sub>O<sub>3</sub> as outer zone materials exhibit relatively high efficiencies in soft x-ray, especially in water window (270–530 eV).

### 3. Fabrication of the compound Kinoform/Fresnel zone plate

The fabrication of the compound Kinoform/Fresnel zone plates was carried out in two steps. In step 1, the dielectric Kinoform zone plate with the outermost zone-width ( $D_r$ ) as 30 nm was first replicated by 3D greyscale electron beam lithography (GS-EBL) [27] in SiO<sub>x</sub>-based hydrogen silsesquioxane (HSQ). To achieve the parabolic shape for the zones as illustrated in figure 1(a), exposure dose distributions (see details in figure S1) were calculated by software of TRACER and LAB, delivered by GenLsys Ltd, following the desired zone profiles. The lens pattern is divided into rings with the width of 5 nm, and each of them is allocated with a specific exposure dose according to the dose distribution curve. Greyscale proximity effect correction (GS-PEC) [27] was also applied to maintain the sloping shape of the Kinoform zones for inner zones. A 350 nm thick HSQ was spin-coated on a 100 nm thick Si<sub>3</sub>N<sub>4</sub> membrane, followed by a soft bake in oven at 180 °C for 2 min. Greyscale exposure using the calculated dose distribution (see in supplement 1) was carried out by a beam-writer, JBX-6300 FS at 100 kV with an e-beam of 7 nm in diameter and 500 pA as the beam current. Hot developing (50 °C) in TMAH: H<sub>2</sub>O (1:3) for 4 min was applied to ensure the clearance of the residual resist [28]. Then the sample was rinsed in de-ionized water for 30 s and dried gently with compressed nitrogen gas. Figure 3(a) presents the fabricated HSQ-Kinoform zone plate with the diameter of 100  $\mu\text{m}$  and the outermost zone width of 30 nm at low magnification of the SEM, and figure 3(b) presents the SEM image of the inner zones with Kinoform-like profile.

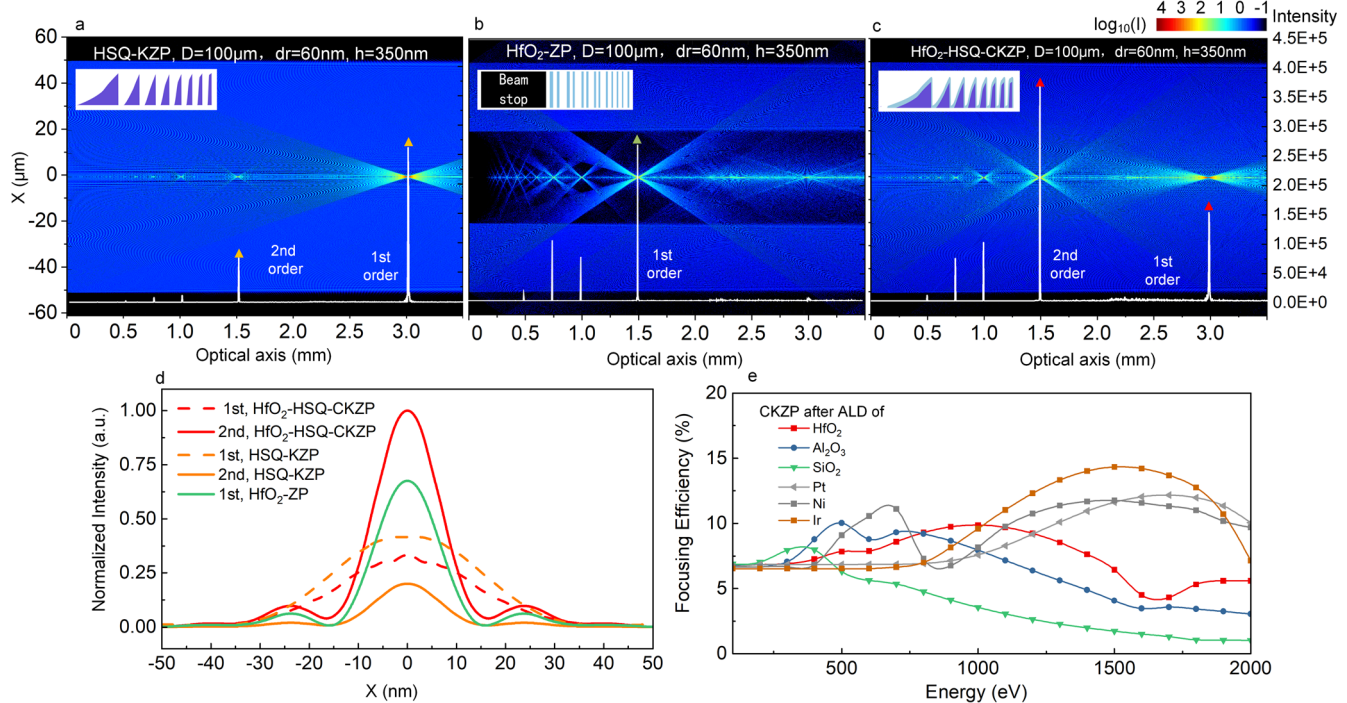


**Figure 2.** The wavefield propagation through the HSQ-KZP, the HfO<sub>2</sub>-ZP and the HfO<sub>2</sub>-HSQ-CKZP. The diameter of CKZPs is 100  $\mu\text{m}$  with a thickness of 350 nm. The outmost period is 60 nm. The thickness of the HfO<sub>2</sub> layer is 15 nm. The detailed lens profiles can be found in supplement. Wavefield propagation in free space was numerically calculated by the beam propagation method with x-ray energy of 1200 eV. (a)–(c) 2D intensity distributions in HSQ-KZP, HfO<sub>2</sub>- ZP and HfO<sub>2</sub>-HSQ-CKZP, respectively. The 1D intensity curve along the central optical axis (white solid line) is presented in the insets. (d) The normalized intensities of the 1st and the 2nd order focal spots of the two lenses, respectively. (e) The focusing efficiency calculation by BPM method for HSQ-KZP coated with a high refractive index film by ALD with the thickness of 15 nm. The zone height is fixed at 350 nm.

The outer zones are rectangularly shaped as presented in figures 3(c), (d), where the outermost line-width is 15 nm with a pitch of 60 nm.

In step 2, a 15 nm thick HfO<sub>2</sub> was coated on the surfaces of the HSQ-Kinoform zones by atomic layer deposition [29, 30]. By this way, a HfO<sub>2</sub>-based binary zone plate with the outermost zone-width of 15 nm is formed in region-III, as presented in figure 3(e) for the top view as well as in figure 3(f) for the tilted view of 45°. The measured height of the zones is 350 nm, corresponding to the aspect ratio of 23:1 for the outmost zones. Smooth surface after ALD is observed in the SEM photos, indicating high deposition quality. Additional ribs were facilitated for zones with widths below 150 nm to avoid collapsing. Through the two-step process, the proposed compound Kinoform/Fresnel zone plate with 15 nm resolution was fabricated.

#### 4. Imaging/focusing by the dielectric compound Kinoform/Fresnel zone plate

Optical characterizations of the fabricated compound HSQ-Kinoform/HfO<sub>2</sub>-zone plate was carried out in Shanghai Synchrotron Radiation Facilities (SSRFs), using an in-house developed scanning transmission x-ray microscopes (STXMs) in the beamline of BL08U1A. An order-sorting aperture was

used to select the focus order. The standard testing sample (an in-house made Siemens star in Au with the minimum feature size of 15 nm in the center) was mounted on a piezoelectric positioning stage for high-precision scanning. An x-ray detector was located behind the sample to collect the transmitted light.

Figure 4 presents the soft x-ray imaging results by the fabricated compound Kinoform/Fresnel zone plate at 1200 eV for the Siemens star. Figures 4(a)–(b) is the SEM and the STXM image, respectively, for the whole testing specimen. In this particular case, STXM scanning was undertaken with the step size of 100 nm. Detailed comparisons between images by SEM and STXM are presented in figures 4(c)/figure 4(d) and in figures 4(e)/figure 4. The structural features in STXM images precisely match those in SEM ones. According to the intensity data of each pixel of the STXM image, three-dimensional topography of the Siemens star was reconstructed using the intensity decay formula, as shown in figures 4(g), (h), trying to reflect the image feature in three dimensions (3D). Both 2D and 3D images clearly show the 15 nm wide lines in the center of the Siemens star be clearly resolved with high contrast. The imaging results demonstrated above verify the successful imaging at the 15 nm resolution by the compound Kinoform/Fresnel zone plate developed in this work.

The focusing capability of the fabricated compound Kinoform/Fresnel zone plate was also characterized by the

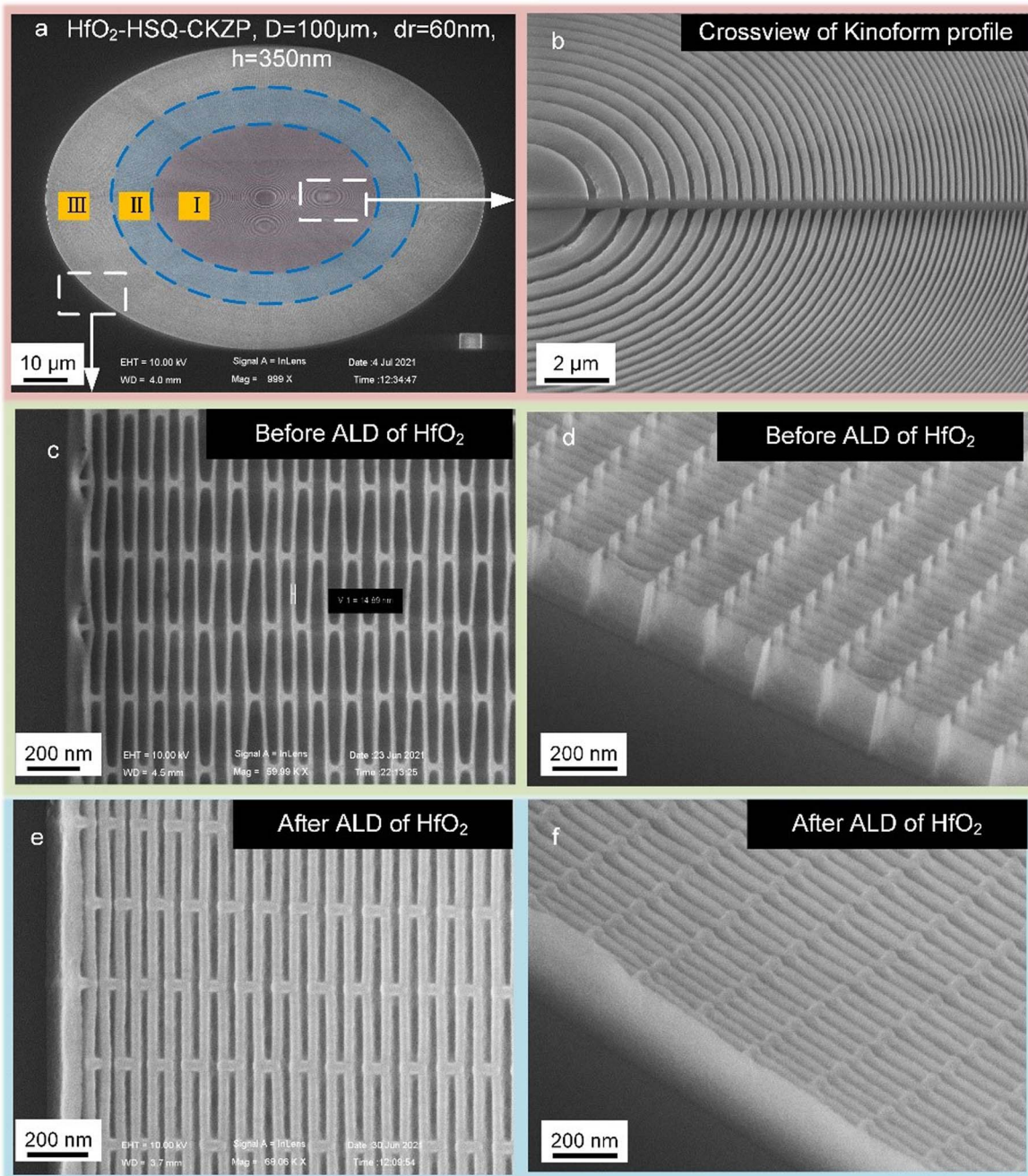


**Figure 3.** Scanning electron micrographs of a zone-doubled  $\text{HfO}_2\text{-HSQ-CKZP}$ . (a) the overviews of  $\text{HfO}_2\text{-CKZP}$  lens with the diameter of  $100\ \mu\text{m}$ ,  $\text{Dr} = 60\ \text{nm}$ ,  $h = 350\ \text{nm}$  and its effective outmost zone width of  $15\ \text{nm}$ . Region-I:  $0 < \text{radius} < 25\ \mu\text{m}$ ; Region-II:  $25\ \mu\text{m} < \text{radius} < 35\ \mu\text{m}$ ; Region-III:  $35\ \mu\text{m} < \text{radius} < 50\ \mu\text{m}$ . (b) The micrographs by SEM for the cross-sectional view at the tilt of  $45^\circ$  of the  $\text{HfO}_2\text{-HSQ-CKZP}$ . Kinoform profiles can be observed. (c)–(d)  $15\ \text{nm}$ -wide lines made of HSQ resist in the outmost area before  $\text{HfO}_2$  coating. (e)–(f) The close-up view of the replicated  $\text{HfO}_2\text{-HSQ-CKZP}$  after  $\text{HfO}_2$  coating.

line-edge scanning method. The focusing spot dimension was quantitatively measured by scanning the focused light across the edges of the Siemens star. The scanning area is  $5 \times 5\ \mu\text{m}^2$  with the step size of  $2.5\ \text{nm}$  and the dwell time of  $1\ \text{ms}$  in the x-ray energy of  $1200\ \text{eV}$ . Figures 5(a)–(c) presents the scanned curves, obtained by scanning in both vertical and horizontal direction, using the compound HSQ-Kinoform/ $\text{HfO}_2$  Fresnel zone plate. The dimensions of the focus spot are obtained from

the full width at half maxima (FWHM) of the scanned curves, which is  $15.5\ \text{nm}$  in horizontal direction (figure 5(b)) and  $15.8\ \text{nm}$  in vertical direction (figure 5(c)). The same measurement was repeated on another compound HSQ-Kinoform/ $\text{Al}_2\text{O}_3$ -Fresnel zone plate, as shown in figures 5(d)–(f). The FWHM of  $17.4\ \text{nm}$  in horizontal directions (figures 5(e)) and  $16.8\ \text{nm}$  in vertical directions (figure 5(f)) was observed. Figure 5(a) and (d) are the STXM images for the two compound Kinoform/Fresnel zone

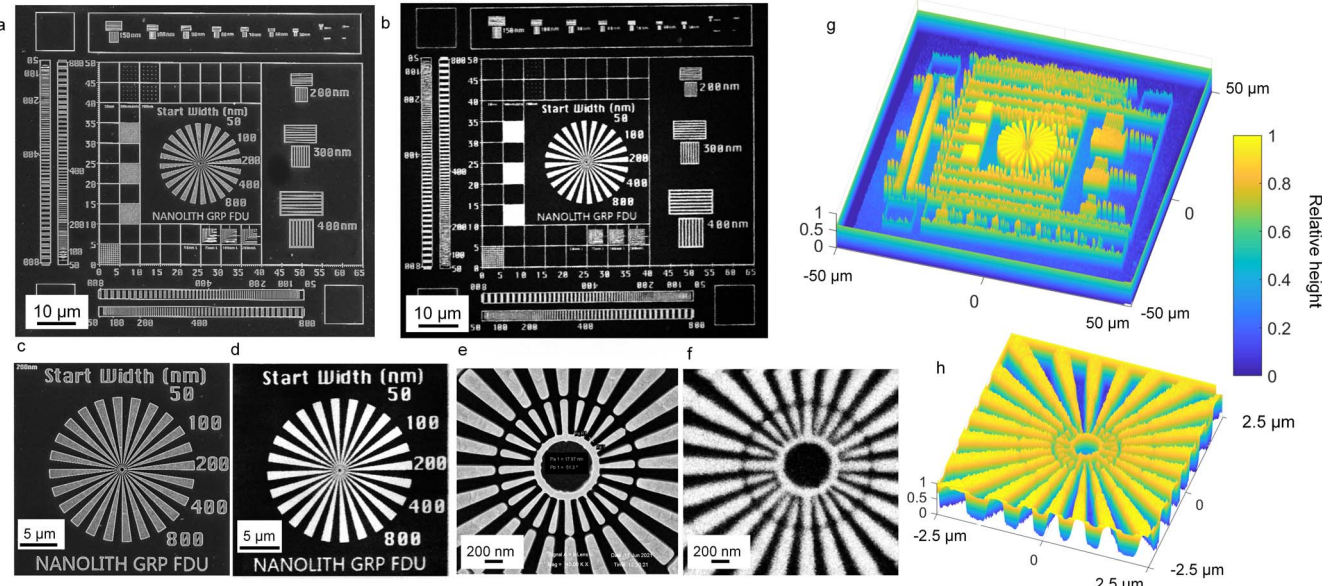


**Figure 4.** Results of soft x-ray imaging tests. (a) The SEM image (left) of the in-house made Siemens star with the resolution of 15 nm. b, the soft x-ray image of the same target by the developed HfO<sub>2</sub>-HSQ-CKZP lens. (c)–(f) The SEM image and the soft x-ray STXM image of the magnified central part of the Siemens star, using the fabricated HfO<sub>2</sub>-HSQ-CKZP. 15 nm lines can be clearly resolved with a good contrast. (g)–(h) The image of three-dimensional topography of the test card reconstructed using the intensity decay formula.

plates, respectively. No sign of focal spot distortion was observed for both compound lenses.

Finally, focusing efficiencies in the energy range of 0.4–1.5 keV were measured for both the compound HSQ-Kinoform/HfO<sub>2</sub>-zone plate and the HSQ-Kinoform/Al<sub>2</sub>O<sub>3</sub>-zone plate. Figure 5(g) presents the measured efficiencies and the theoretical ones for comparison. For the compound HSQ-Kinoform/HfO<sub>2</sub>-zone plate, the maximum efficiency was measured to be 7.8% at 1200 eV, which is about 88% of the theoretical figure. The other compound HSQ-Kinoform/Al<sub>2</sub>O<sub>3</sub>-zone plate also exhibits the peak efficiency of 6.5% at 700 eV. In a broad energy range from 500 to 1500 eV, the efficiencies of both lenses are over 5%, which is promising in practical use in sub-20 nm resolution STXMs. Furthermore, both two kinds of compound lenses are able to stand soft X ray radiation for at least 12 h. To further verify the gain in efficiency of CKZP, focusing efficiency of KZP, Kinoform lens (KF), CKZP, ZP and zone-doubled zone plate (CZP) are calculated respectively, as shown in figure 5(h)–(i). Due to the nonideal parabolic profile of the zones as illustrated in figure 1, the efficiency of 2nd foci at 1.5 mm for HSQ-KZP is stronger than that of both HSQ-ZP and HSQ-KF, which therefore makes contributions to the efficiency of HfO<sub>2</sub>-HSQ-CKZP. For conventional HfO<sub>2</sub>-HSQ-CZP (zone-doubled Fresnel zone plate), however, this benefit from overlayed HfO<sub>2</sub>-ZP and HSQ-ZP is not significant. From the curve of efficiency verses zone thickness,  $\pi$  rad phase shift for HfO<sub>2</sub> and HSQ appears in 500 nm and 1400 nm, respectively, whereas the height of fabricated lenses in this study is 350 nm due to the limitation of nanofabrication capability, which provides 0.7 $\pi$  and 0.25 $\pi$  rad phase shift for HfO<sub>2</sub> and HSQ, respectively. The limited zone

height of HSQ-KF is not optimal for the performance and therefore suppress the gain of HSQ-KZP to the efficiency of CKZP. As the zone height increases to 700 nm (figure 5(i)), the 1.4 $\pi$  rad phase shift for HfO<sub>2</sub> and 0.5 $\pi$  rad phase shift for HSQ are at their optimal combination so that the efficiency of HfO<sub>2</sub>-HSQ-CKZP reaches the highest, compared with other kinds of lenses. This benefit exists as the resolution of CKZP reaches to 10 nm. It is worth mentioning that the increase in height (from 350 to 700 nm) results in phase accumulation but the accompanying energy loss [31, 32] is not vital due to the low losses of the dielectric material in this energy band. The CKZP with special structure performs better on focusing than zone-doubled Fresnel zone plate over a wide energy range, however, the phase loss due to the height limitation and phase mismatch between two materials need to be alleviated to further improve the focusing efficiency.

## 5. Conclusions

To achieve both high resolution and high efficiency for the focusing/imaging in soft x-ray, a compound Kinoform/Fresnel zone plate lens by combining an HSQ based Kinoform zone plate with a HfO<sub>2</sub> based Fresnel zone plate was developed using greyscale electron beam lithography and atomic layer deposition. 15 nm resolution with the focusing/imaging efficiency of 7.8% at 1200 eV was demonstrated by both theoretical calculations using BPM method and optical characterization by scanning transmission x-ray microscope (STXM). The enhanced efficiency should be credited to the following exercises. First, the beamstop was replaced by Kinoform zones in the center. Second, the

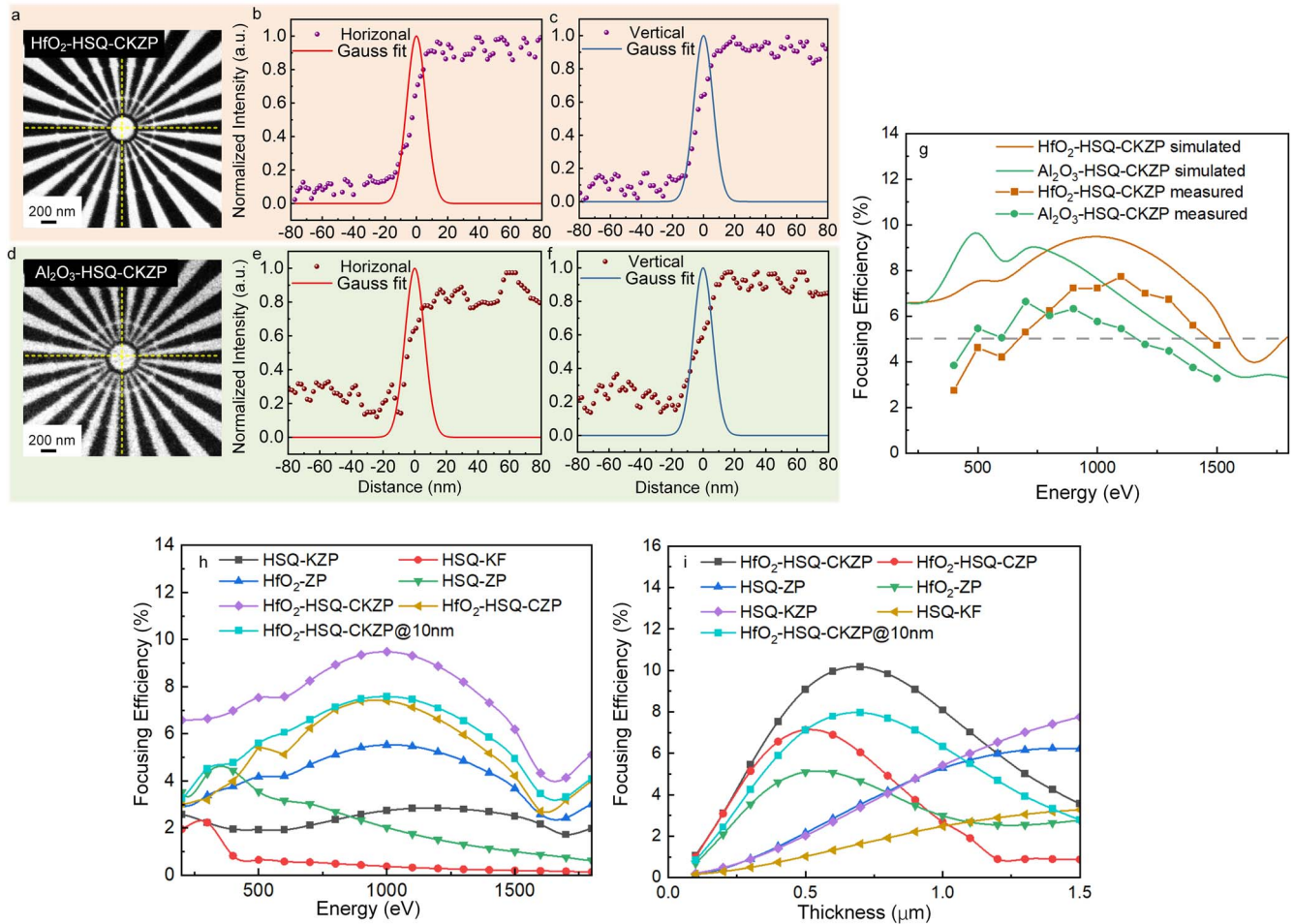


**Figure 5.** Results of soft x-ray focusing and efficiency tests. (a)–(f) Focused beam profiles of the  $\text{HfO}_2\text{-HSQ-CKZP}$  and the  $\text{Al}_2\text{O}_3\text{-HSQ-CKZP}$ , respectively, measured by the knife-edge scan method. The dotted-lines represent the raw data of scanned curves and the solid lines are the first order derivative of the measured scanning curves. (g) the comparison between the measured focusing efficiencies of  $\text{HfO}_2\text{-HSQ-CKZP}$  and the  $\text{Al}_2\text{O}_3\text{-HSQ-CKZP}$  and the theoretical ones by the BPM approach. (h) The focusing efficiencies changing with photon energy, calculated by BPM method for KZP, Kinoform lens(KF), CKZP, ZP and zone-doubled zone plate (CZP), respectively. The lens resolution is 15 nm and the focal length is 1.5 mm. The efficiency of  $\text{HfO}_2\text{-HSQ-CKZP}$  with 10 nm resolution is also calculated. (i), The focusing efficiency as the function of the thickness, calculated by BPM method for KZP, Kinoform lens(KF), CKZP, ZP and CZP, respectively, for the photon energy of 1200 eV.

focusing efficiency of the combined zone plate is the superposition of that from both the HSQ-Kinoform zone plate and the  $\text{HfO}_2$ -zone plate. Third, low loss dielectric films instead of metallic ones were employed for the zones. The achievements made in this work provide an effective solution to both high resolution and high efficiency in the development of soft x-ray nanoprobe technique.

## Funding

Shanghai STCSM project (Grant No. 19142202700); National Natural Science Foundation of China (Grant Nos. U1732104, 61927820, 11875316, U1832146).

## Acknowledgments

The authors thank the BL08U1A beamline and BL15U1 beamline of the Shanghai Synchrotron Radiation Facility for providing the beamtime.

## Data availability statement

The data that support the findings of this study are available upon reasonable request from the authors.

## Disclosures

The authors declare no conflicts of interest.

## Supplemental document

See Supplement 1 for supporting content.

## ORCID iDs

Yifang Chen <https://orcid.org/0000-0001-8918-515X>  
 Hongliang Lu <https://orcid.org/0000-0003-2398-720X>

## References

- [1] Barth R, Staier F, Simpson T, Mittler S, Eisebitt S, Grunze M and Rosenhahn A 2010 Soft x-ray holographic microscopy of chromosomes with high aspect ratio pinholes *J. Biotechnol.* **149** 238–42
- [2] Chen R et al 2021 Tunable room-temperature ferromagnetism in Co-doped two-dimensional van der Waals ZnO *Nat. Commun.* **12** 3952
- [3] Dehlinger A, Seim C, Stiel H, Twamley S, Ludwig A, Kordel M, Grotzsch D, Rehbein S and Kanngiesser B 2020 Laboratory soft x-ray microscopy with an integrated visible-light microscope-correlative workflow for faster 3D cell imaging *Microsc. Microanal.* **26** 1124–32
- [4] Ferreira Sanchez D et al 2021 Spatio-chemical heterogeneity of defect-engineered metal-organic framework crystals revealed by full-field tomographic x-ray Absorption spectroscopy *Angew. Chem. Int. Ed. Engl.* **60** 10032–9
- [5] Holler M, Guizar-Sicairos M, Tsai E H, Dinapoli R, Muller E, Bunk O, Raabe J and Aepli G 2017 High-resolution non-destructive three-dimensional imaging of integrated circuits *Nature* **543** 402–6
- [6] Le P T P et al 2019 Tailoring vanadium dioxide film orientation using nanosheets: a combined microscopy, diffraction, transport, and soft x-ray in transmission study *Adv. Funct. Mater.* **30**
- [7] Yamamoto K et al 2017 Influence of the skin barrier on the penetration of topically-applied dexamethasone probed by soft x-ray spectromicroscopy *Eur. J. Pharm. Biopharm.* **118** 30–7
- [8] Chao W, Harteneck B D, Liddle J A, Anderson E H and Attwood D T 2005 Soft x-ray microscopy at a spatial resolution better than 15 nm *Nature* **435** 1210–3
- [9] Keskinbora K, Sanli U T, Baluktsian M, Grevent C, Weigand M and Schutz G 2018 High-throughput synthesis of modified Fresnel zone plate arrays via ion beam lithography *Beilstein J. Nanotechnol.* **9** 2049–56
- [10] Reinsch J, Lindblom M, Bertilson M, von Hofsten O, Hertz H M and Holmberg A 2011 13 nm high-efficiency nickel-germanium soft x-ray zone plates *J. Vac. Sci. Technol. B* **29**
- [11] Sanli U T et al 2018 3D nanofabrication of high-resolution multilayer fresnel zone plates *Adv. Sci. (Weinh)* **5** 1800346
- [12] Vila-Comamala J, Gorelick S, Farm E, Kewish C M, Diaz A, Barrett R, Guzenko V A, Ritala M and David C 2011 Ultra-high resolution zone-doubled diffractive x-ray optics for the multi-keV regime *Opt. Express* **19** 175–84
- [13] Marschall F, Vila-Comamala J, Guzenko V A and David C 2017 Systematic efficiency study of line-doubled zone plates *Microelectron. Eng.* **177** 25–9
- [14] Yurgens V, Koch F, Scheel M, Weitkamp T and David C 2020 Measurement and compensation of misalignment in double-sided hard x-ray Fresnel zone plates *J. Synchrotron Radiat.* **27** 583–9
- [15] Rösner B et al 2020 Soft x-ray microscopy with 7 nm resolution *Optica* **7**
- [16] Vila-Comamala J, Jefimovs K, Raabe J, Pilvi T, Fink R H, Senoner M, Maassdorf A, Ritala M and David C 2009 Advanced thin film technology for ultrahigh resolution x-ray microscopy *Ultramicroscopy* **109** 1360–4
- [17] Rösner B et al 2018 Exploiting atomic layer deposition for fabricating sub-10 nm x-ray lenses *Microelectron. Eng.* **191** 91–6
- [18] Aristov V, Grigoriev M, Kuznetsov S, Shabelnikov L, Yunkin V, Weitkamp T, Rau C, Snigireva I, Snigirev A and Hoffmann M J A P L 2000 X-ray refractive planar lens with minimized absorption *Appl. Phys. Lett.* **77** 4058–60
- [19] Mohacsi I, Karynen P, Vartiainen I, Guzenko V A, Somogyi A, Kewish C M, Mercere P and David C 2014 High-efficiency zone-plate optics for multi-keV x-ray focusing *J. Synchrotron Radiat.* **21** 497–501
- [20] Sun Y-L, Dong W-F, Niu L-G, Jiang T, Liu D-X, Zhang L, Wang Y-S, Chen Q-D, Kim D-P and Sun H-B 2014 Protein-based soft micro-optics fabricated by femtosecond laser direct writing *Light: Sci. Appl.* **3** e129-e
- [21] Xie J, Liang S, Liu J, Tang P and Wen S 2020 Near-zero-sidelobe optical subwavelength asymmetric focusing lens with dual-layer metasurfaces *Ann. Phys.* **532**
- [22] Yu J, Bai Z, Zhu G, Fu C, Li Y, Liu S, Liao C and Wang Y 2020 3D nanoprinted kinoform spiral zone plates on fiber facets for high-efficiency focused vortex beam generation *Opt. Express* **28** 38127–39
- [23] Simpson M J and Michette A G 2010 Imaging properties of modified fresnel zone plates *Opt. Acta: Int. J. Opt.* **31** 403–13
- [24] Roey J V, Donk J and Lagasse P E 1981 Beam-propagation method: analysis and assessment *J. Opt. Soc. Am* **71**
- [25] Tong X, Chen Y, Xu Z, Li Y, Xing Z, Mu C, Zhao J, Zhen X, Mao C and Tai R 2022 Trapezoid-kinoform zone plate lens —a solution for efficient focusing in hard x-ray optics *J. Synchrotron Radiat.* **29** 386–92
- [26] Vila-Comamala J, Wojcik M, Diaz A, Guizar-Sicairos M, Kewish C M, Wang S and David C 2013 Angular spectrum simulation of x-ray focusing by fresnel zone plates *J. Synchrotron Radiat.* **20** 397–404
- [27] Tong X, Xu C, Zhu J, Mao C, Zhen X, Huang W and Chen Y 2020 A study of greyscale electron beam lithography for a 3D round shape Kinoform lens for hard x-ray optics *Microelectron. Eng.* **234**
- [28] Chen Y 2015 Nanofabrication by electron beam lithography and its applications: a review *Microelectron. Eng.* **135** 57–72
- [29] Li Y C, Li X X, Zeng G, Chen Y C, Chen D B, Peng B F, Zhu L Y, Zhang D W and Lu H L 2021 High optoelectronic performance of a local-back-gate ReS<sub>2</sub>/ReSe<sub>2</sub> heterojunction phototransistor with hafnium oxide dielectric *Nanoscale* **13** 14435–41
- [30] Zhang Y, Tao J J, Chen H Y and Lu H L 2021 Preparation of single crystalline AlN thin films on ZnO nanostructures by atomic layer deposition at low temperature *Nanotechnology* **32**
- [31] Gorelick S, De Jonge M D, Kewish C M and De Marco A 2019 Ultimate limitations in the performance of kinoform lenses for hard x-ray focusing *Optica* **6**
- [32] Feng B, Chen Y, Sun D, Yang Z, Yang B, Li X and Li T 2021 Precision integration of grating-based polarizers onto focal plane arrays of near-infrared photovoltaic detectors for enhanced contrast polarimetric imaging *International Journal of Extreme Manufacturing* **3**